Biomedical Letters ISSN 2410-955X DOI: https://doi.org/10.47262/BL/8.2.20220628

Research article
2022 | Volume 8 | issue 2 | Pages 184-195

ARTICLEINFO

Received
April 02, 2022
Revised
May 11 2022
Accepted
July 03, 2022

***Corresponding Author**
Yasmeen Bibi

E-mail
yasmeen577@yahoo.com

Keywords
Metal complexes
Absorption spectra
^{1}H-NMR
SEM with EDX
Antimicrobial activities

How to Cite
Bibi Y, Wahab A, Shah SN, Satar S, Hassan A, Sherwani SK, Shah SA. Characterization of metal (Mg, Ni & Zn) complexes with β-sitosterol for antimicrobial studies. Biomedical Letters 2022; 8(2):184-195.

Scan QR code to see this publication on your mobile device.

Open Access

Characterization of metal (Mg, Ni & Zn) complexes with β-sitosterol for antimicrobial studies

Yasmeen Bibi [1]*, Aneela Wahab[1], S. Naseem Shah[2], Samina Satar[1], Atya Hassan[1], Sikandar Khan Sherwani[3], Syed Ahsan Shah[4]

[1]Department of Chemistry, Federal Urdu University of Arts, Science and Technology, Karachi, Pakistan
[2]Department of Physics, Federal Urdu University of Arts, Science and Technology, Karachi, Pakistan
[3]Department of Microbiology, Federal Urdu University of Arts, Science and Technology, Karachi, Pakistan
[4]Department of Botany, Hazara University, Mansehra, Pakistan

Abstract

The metal complexes of Mg (II), Ni (II), and Zn (II) with β- sitosterol were synthesized and the obtained complexes were characterized by various techniques such as elemental analysis, Infrared Spectroscopy (IR), UV Visible Spectroscopy (UV VIS), Proton Nuclear Magnetic Resonance (1H-NMR), Electron Dispersive X-ray Spectroscopy (EDX), Scanning Electron Microscopy (SEM) and Thermo Gravimetric Analysis (TGA). From the analytical data, the stoichiometry of all the complexes was found to be a 1:2 (metal: ligand) ratio with the general formula ML2X. The IR spectral data predict that the βs behave as a bidentate ligand with a hydroxyl group (OH) and C=C (double bond) groups pointing towards the central metal ion. The Absorption spectra showed an octahedral geometry of the complexes. The EDX features indicated that the desired elements along with their mass percentage ratio are present in the metal complexes. The ligand and complexes were screened for their antibacterial, antifungal and antioxidant activities. The metal ions present in the complexes accelerate the anti-microbial activity and they are more effective than ligands in terms of their biological activity which gives them the opportunity for use in medical practice.

Introduction

The metal complexes have versatile applications in the field of medical sciences. These are commonly used for catalysis, agrochemical and biological activities [1] such as anti-proliferative, anti-inflammatory, and anti-arthritic [2-4] and therapeutic agents [5]. The metal complexes are potentially more important for the body and less toxic compared to drug intake. The drug intake possessed more pharmacological and toxicological effects as compared to metal complexes [6]. Besides the drugs, the pharmacological properties of metal complexes depend upon the formation of ions, the structure of the complex and its ligands. These features of metal complexes are important because they can easily reach the target site in the body for proper treatment. Certain metal ions are responsible for killing the bacteria either by penetrating these ions into bacteria by deactivating the enzymes or some metal ions able to produce hydrogen peroxide [7]. The coordination complexes of platinum such as cisplatin, carboplatin, and oxaliplatin are chemo-therapeutic agents to treat cancer [7,8]. β-sitosterol is a naturally occurring sterol found in plants [9-12] and has been proven to be a safe, effective nutritional supplement and has shown amazing potential benefits in many applications [13-15]. It has been reported that β-sitosterol is an effective compound for chemopreventive drugs [16] and another study showed that β-sitosterol stimulates antioxidant enzymes and has good reactive oxygen species [17].

In this study, β-sitosterol (ligand) and Mg, Ni, and Zn were used for the formation of the complexes. It has been reported that the biological activities of the complexes are usually enhanced upon metal complexation [18]. There was a lack of information in the literature about the formation of metal complexes with β-sitosterol. In this research, we investigate the role of metal complexes with β-sitosterol to study antimicrobial and antioxidant activity.

Materials and Methods

For the synthesis of metal complexes, β-sitosterol, Magnesium (II) acetate tetra hydrated, Nickel (II) nitrate hexahydrate, and Zinc (II) acetate tri hydrated of analytical grade (Merck) were used. For weighing, Denver Instrument, TP- 214 was used. The melting point was determined on the Gallen Kamp apparatus. Thin-layer chromatography (TLC) was performed on pre-coated silica gel (GF-254). The elemental analysis of the complexes was carried out by Perkin Elmer (2400 CHN) elemental analyzer. For IR spectroscopy, a Jasco-302-A spectrophotometer was used. The absorption spectra of the complexes were recorded on a UV/Visible spectrophotometer (Shimadazu-1800). Brucker spectrometer (operating at 500 MHz) was used to obtain the ^{1}H-NMR spectra of the samples. The morphological features and the mass percentage of each element were determined by SEM along with EDX (JSM 6380 A Joel, Japan) instrument. The complexes' TG analysis was studied using Perkin-Elmer Thermogravimetric analyzer (TGA 7).

Synthesis of metal complexes

The metal complexes were synthesized by adding 0.1 M (0.214, 0.290, and 0.219 g) metal salts of Mg, Ni, and Zn respectively to the ligand (0.2 M, 0.829 g) in a mole ratio of 1:2 by dissolving in 20 mL anhydrous DMF. The reaction mixture was heated up to 140±10^{o}C with continuous stirring in an inert atmosphere for about 15 minutes. The obtained solution was kept overnight at room temperature. The solid product was obtained after filtering, washing, and drying in a vacuum**.**

For culturing bacterial strains, Muller Hinton agar and Muller Hinton broth were used as the media. The antibacterial activity of the complexes under study against the test organisms was measured by applying the agar-well technique. To recharge the bacterial culture, the autoclaved Muller Hinton broth was used. After this, the well was punched into Muller Hinton Agar and aliquots (10 µl) of culture were transferred into the wells [19, 20]. 10 mg/ml solution of the sample was used for screening antibacterial activity. The temperature of all plates was maintained up to 28±2 ^{0}C for 48 h in the incubator and measurement for the diameter of the zone of inhibition was performed by Vernier caliper. Whereas Gentamicin antibiotic was served as standard [21].

Anti microbial assay

Seaboard dextrose agar (SDA) was used as the media for the development of fungal strains [22]. Antifungal activity of all the samples was recorded by applying the agar-well method. Preparation of fungal spore suspension was carried out in autoclaved distilled water and transferred aseptically into each SDA plate [23]. 10 mg/mL solution of the sample was used for screening antifungal activity. The temperature of all plates was maintained up to 28±2 ^{0}C for 48 h in the incubator and measurement for the diameter of the

zone of inhibition was performed subsequently. Gresiofulvin antifungal agent served as a standard. The Micro broth dilution method was used to determine the minimum inhibitory concentration (MIC) by using a 96-well microtitre plate [23]. In this process, two-fold serial dilutions of extracts were prepared in 100 µl broth. After this, 10 µl of refreshed culture were matched and 0.5 Mac Farland index was added to each well. One well served as culture control and the other well served as antifungal agent control. The temperature of the microtitre plate was maintained up to 37 ^{0}C for 24 hours. The values of MIC for the complexes were read and it was also noted that the well showed no visible growth.

Antioxidant assay

Antioxidant activities of ligand and its complexes with metal were performed by using a 1, 1-diphenyl-2-picrylhydrazyl (DPPH) assay [24]. The reaction mixture comprised 1mL (0.5-0.0156 mg/mL) of the test sample and 2 mL of methanolic solution of DPPH (100 µM) that was dissolved in dimethyl sulfoxide (DMSO). After half, an hour of incubation change in absorption was recorded at 520 nm with the help of a spectrophotometer. The control contained 1 mL of DMSO, instead of the test sample [25]. Radical Scavenging activity was expressed in terms of percentage scavenging activity (% RSA). Ascorbic acid and Butylated hydroxyl toluene (BTH) served as reference compounds.

Results and Discussion

Physical characteristics

The complexes of metals (Mg, Ni, and Zn) with β-sitosterol were obtained by using DMF as a solvent under the inert condition with continuous stirring and heating (130-150^{o}C). During the complexation of Mg with βs, the color changed from colorless to yellow, whereas for βs -Ni complex, the color changed from light green to deep green and for βs - Zn complex, milky white color was observed (**Table 1)**. Elemental analysis shows the percentage of Carbon and hydrogen in complexes.

The IR spectrum of the ligand (βs) showed the OH band at 3400 cm^{-1} and C=C at 1650 cm^{-1} (**Table 2**) These two bands were shifted to lower frequency (OH band appeared at 3131 – 3383 cm^{-1} and the C=C band at 1559 -1607 cm^{-1}) in all the metal complexes indicating that metal may be lie between OH and C=C bond of the ligand. Besides these bands, IR spectra of all the complexes also exhibited weak bands in the region 430-491 cm^{-1} assigned to metal-oxygen (M-O) stretching vibration [26-28]. This band further justifies the involvement of the oxygen atom of the ligand in the metal ion [29].

Electronic absorption spectra

The UV/VIS spectra of ligand (βs) and its metal complexes are shown in **Fig. 1**. The spectral data of βs and βs–Mg, βs–Ni and βs–Zn are tabulated in **Table 3.** The two major bands of ligand (βs) at 47619.05(C=C) and (OH) 35714.29 cm^{-1} are observed. These bands shifted to a lower frequency in all the metal complexes providing evidence for the coordination of metal ions through OH and C=C of the ligand. The βs–Mg complex is found to be diamagnetic [30, 31] with octahedral geometry**.** Whereas the UV spectrum of βs–Ni complex exhibited three new bands at 26178.01, 15384.62, and 10683.76 cm^{-1} suggesting an octahedral geometry around the metal ion [32]. The βs–Zn complex displays bands of ligand which were shifted to lower frequencies as compared to the corresponding bands in the spectrum of the free ligand, which justify the coordination of the ligand to the metal ion [33-35].

^{1}H NMR spectra

The ^{1}H NMR spectrum of the ligand [36] and its metal complexes were recorded in Deuterated chloroform ($CDCl_3$) and the spectral data are presented in **Table 4.** The remarkable changes in the chemical shift values of H-3, H-6 and OH were observed for all the metal complexes. These protons shifted downfield due to the coordination of metal ions through ligand [37].

Elemental analysis

The elemental composition of all the metal complexes was determined by EDX **(Table 5)**. The EDX scan of ligand (βs) showed carbon (0.277 keV) and oxygen (0.525 keV) as the major constituent **(Fig. 2-a).** In the EDX spectra of the βs-Mg complex, the peak at 1.253 keV was observed representing the features of Mg (**Fig.2-b)**. Notable peaks of Ni at 0.851 and 7.471 keV appeared in the βs-Ni complex (**Fig.2-c**). **Fig.2(d)** shows the peaks at 1.012 and 8.630 keV which indicate the features of Zn. Overall, the appearance of the EDX feature of Mg, Ni, and Zn at their respective KeV correspond quite well with the values reported in EDAX international chart [38].

Table 1: Physical parameters of βs and its complexes with metals.

Sample code	Color	Molecular weight	Temperature (°C)	Yield (%)	Melting Point (°C)	Elemental analysis (%) (Calcd) C	H	Proposed Formula
βs	Colorless	414.71	-	-	140	83.99 (83.97)	12.15 (12.06)	$C_{29}H_{50}O$
βs–Mg	Yellow	1030.94	140	93	230	73.40 (73.41)	11.83 (11.74)	$[MgL_2(H_2O)_2](CH_3COO)_2.H_2O$
βs–Ni	Green	1088.27	140	90	220	66.22 (66.24)	10.93 (10.86)	$[NiL_2(H_2O)_2](NO_3)_2.H_2O$
βs–Zn	White	1054.00	150	95	240	71.79 (71.87)	11.38 (11.31)	$[ZnL_2(H_2O)_2](CH_3COO).H_2O$

Table 2: Infrared vibrational frequencies (cm^{-1}) of βs and its complexes.

Sr. #	Sample code	Functional group OH (cm^{-1})	C=C (cm^{-1})	C-O (cm^{-1})	M-O (cm^{-1})
1	βs	3400	1650	1063	-
2	βs–Mg	3210	1572	1060	482
3	βs–Ni	3355	1559	1060	477
4	βs–Zn	3353	1592	1063	491

Table 3: Electronic spectra of βs and its complexes.

Sr. #	Sample code	λ (nm)	ν (cm^{-1})	Geometry
1	βs	210	47619.05	-
		280	35714.29	
2	βs–Mg	252	39682.54	Octahedral
		384	26041.66	
3	βs–Ni	236	42372.88	Octahedral
		308	32467.53	
		382	26178.01	
		650	15384.62	
		936	10683.76	
4	βs–Zn	230	43478.26	Octahedral
		296	33783.78	

Table 4: ^{1}H-NMR data of βs and its complexes at 500 MHz in $CDCl_3$: δ in ppm J in Hz

S. No	Proton	βs	βs-Mg	βs-Ni	βs-Zn
1	H-3	3.51 (1H, m)	3.85 (1H, m)	3.60 (1H, m)	3.70 (1H, m)
2	H-6	5.30 (1H) (br, s)	5.55 (1H) (br, s)	5.80 (1H) (br, s)	5.60 (1H) (br, s)
3	CH_3-18	0.67 (3H, s)	0.67 (3H, s)	0.69 (3H, s)	0.65 (3H, s)
4	CH_3-19	0.99 (3H, s)	0.99 (3H, s)	0.97 (3H, s)	0.99 (3H, s)
5	CH_3-21	0.92 (3H, d, *J* = 6.2)	0.90 (3H, d, *J* = 6.2)	0.93 (3H, d, *J* = 6.2)	0.92 (3H, d, *J* = 6.2)
6	CH_3-26	0.81 (3H, d, *J* = 6.5)	0.83 (3H, d, *J* = 6.5)	0.80 (3H, d, *J* = 6.5)	0.82 (3H, d, *J* = 6.5)
7	CH_3-27	0.78 (3H, d, *J* = 6.2)	0.78 (3H, d, *J* = 6.2)	0.76 (3H, d, *J* = 6.2)	0.78 (3H, d, *J* = 6.2)
8	CH_3-29	0.84 (3H, t, *J* = 7.2)	0.86 (3H, t, *J* = 7.2)	0.83 (3H, t, *J* = 7.2)	0.85 (3H, t, *J* = 7.2)
9	OH	4.50	5.00	4.95	5.00

Note: br= broad, m= multiplet, s= singlet, t=triplet and J= coupling constant in Hz

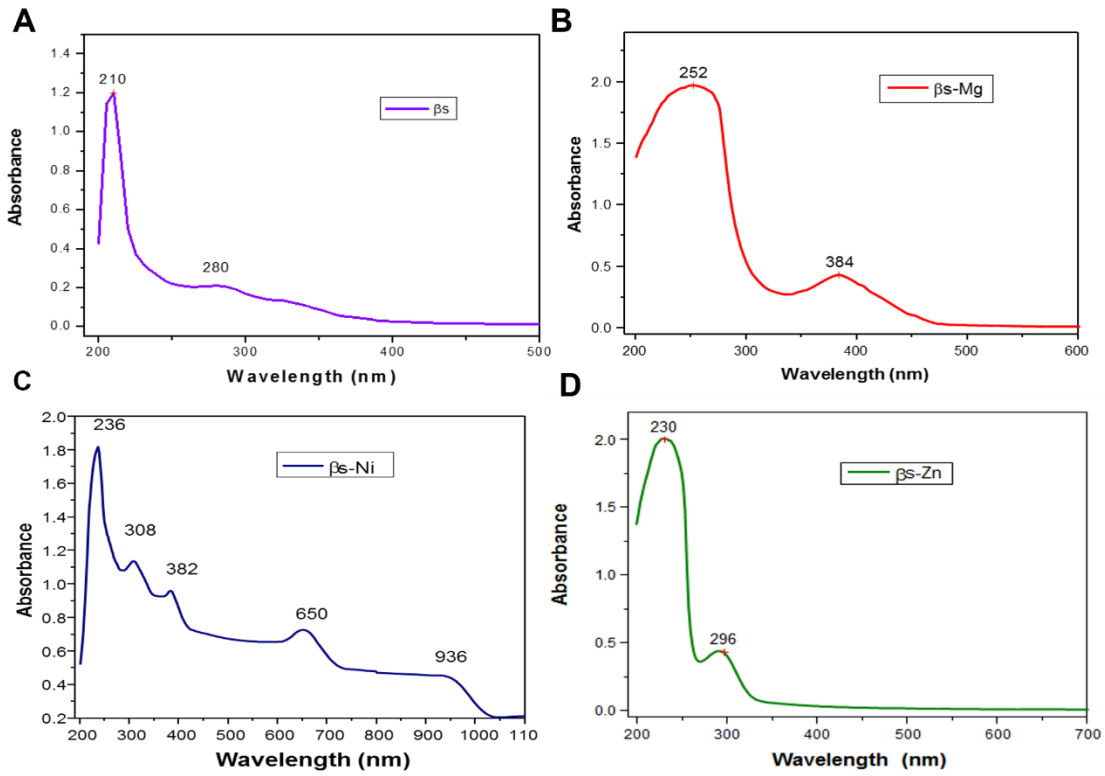

Fig. 1: UV/VIS spectra of (**A**) βs, (**B**) βs–Mg, (**C**) βs–Ni and (**D**) βs–Zn

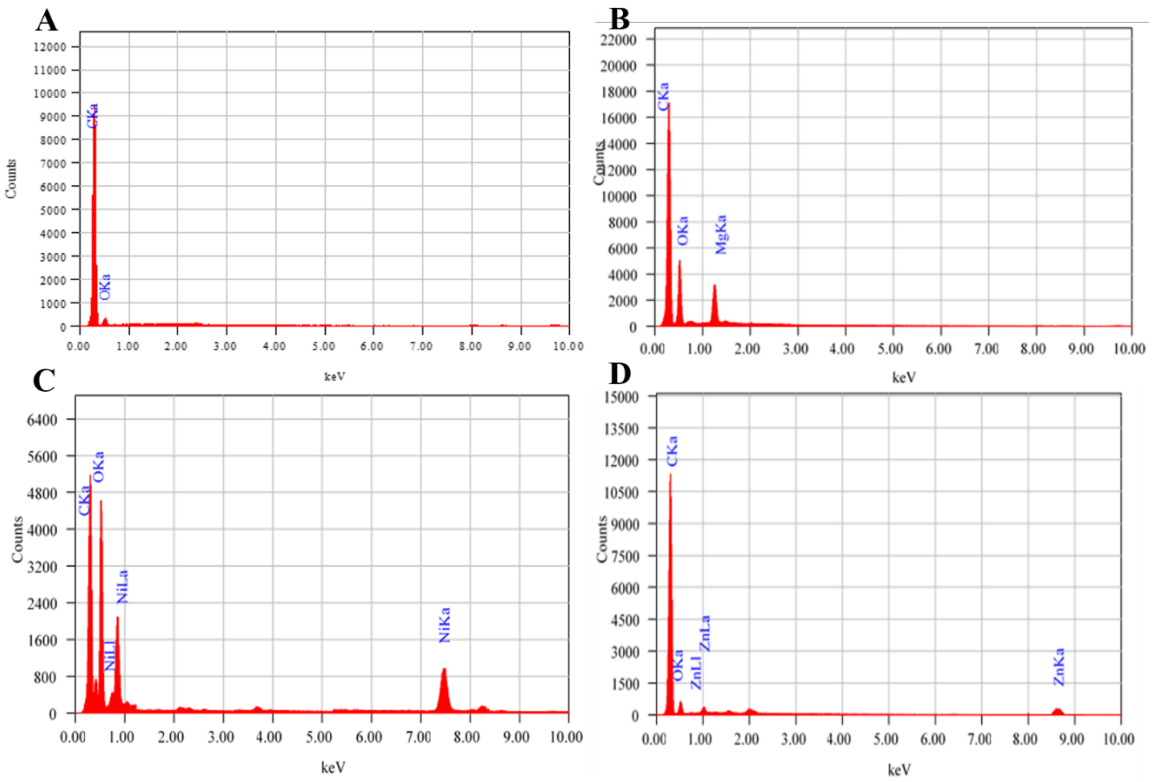

Fig. 2: The EDX results for (**A**) βs, (**B**) βs–Mg, (**C**) βs–Ni and (**D**) βs–Zn

Table 5: The quantitative analysis of EDX results of the βs and its complexes.

S.No	Sample code	Elements	KeV	Mass%	At%
1	βs	C	0.277	83.19	86.83
		O	0.525	16.81	13.17
2	βs-Mg	C	0.277	62.96	71.42
		O	0.525	33.24	27.40
		Mg	1.253	3.80	1.18
3	Bs-Ni	C	0.277	46.38	54.44
		O	0.525	43.88	39.71
		Ni	7.471	9.82	5.85
4	Bs-Zn	C	0.277	62.69	72.17
		O	0.525	30.55	26.40
		Zn	1.012	6.76	1.43

Table 6: TGA data of sterol-metal complexes

Complex	Decomposition Temp. (ºC)	Lost fragment	Weight loss %	
			Observed	Calculated
$[MgL_2(H_2O)_2](CH_3COO)_2.H_2O$	70-120	Loss of two lattice water molecules	3.397	3.415
	120-210	Loss of two coordinated water molecules and loss of two ligands	82.099	82.115
	210-400	Loss of uncoordinated acetate	11.214	11.196
	400-900	Residue of metal oxide	3.901	3.823
$[NiL_2(H_2O)_2](NO_3)_2.4H_2O$	70-120	Loss of four lattice water molecules	6.494	6.580
	120-210	Loss of two coordinated water molecules and loss of two ligands	79.127	79.090
	210-400	Loss of uncoordinated NO_3	11.421	11.332
	400-900	Residue of metal oxide	6.902	6.817
$[ZnL_2(H_2O)_2](CH_3COO).2H_2O$	70-120	Loss of one lattice water molecule	1.720	1.643
	120-210	Loss of two coordinated water molecules and loss of two ligands	79.102	79.035
	210-400	Loss of uncoordinated acetate	10.810	10.776
	400-900	Residue of metal oxide	7.379	7.432

Surface morphology

The surface morphology of the β-sitosterol and its complexes were determined by SEM. Significant changes in the surface morphology were observed due to the interaction of metals with ligands. SEM image of ligand (βs) shows dense and rough surface morphology (see **Fig. 3-a)** and this dense morphology disappeared after the contact of the ligand with metals. Interaction with metals changes the surface morphology in βs-Mg complex **(**see **Fig. 3-b)** plain texture was observed**.** In the case of the βs-Ni complex, projections and cavities-like morphology are observed (see **Fig.3-c**) whereas the βs-Zn complex shows polygon-like texture **(**see **Fig. 3-d).** Overall, the change in the texture of the ligand and its metal complexes is due to the interaction of the metal with the ligand to arrange in the fixed geometry.

Thermal analysis

TGA analysis was carried out under a nitrogen atmosphere and the loss in mass was measured from the ambient temperature up to 1000 ºC. The results obtained through thermal analysis of complexes are tabulated in **Table 6.** Metal complexes show four stages of decomposition. The first stage of decomposition was observed at the temperature range of 70-120 ^{0}C. It indicated the % weight loss of lattice water molecules. The second stage decomposition is obtained in the temperature range of 120-210 ^{0}C corresponding to the loss of coordinated water and ligand molecules [39,40]. The third stage decomposition observed in the range 210-400 ^{0}C is indicative of the loss of the uncoordinated nitrate group in the βs-Ni complex, whereas the loss of acetate group in βs-Mg and βs-Zn complexes. The last stage of decomposition occurred in the temperature range of 400-900 ^{0}C indicating the loss of metal oxide residue. TGA analysis like other spectral analyses further confirmed the proposed structure of all metal complexes as shown in **Fig. 4.**

Chemical structure of complexes

All the synthesized complexes of β-sitosterol with metals have the general formula $ML_2X_2.x\ H_2O$ where

M= Mg, Ni and Zn, L= βs and X= NO_3^- and CH_3COO^-. From the above spectral analysis (UV-Visible, IR) the proposed structure of all the metal complexes is shown in **Fig. 4.**

Biological structure of complexes

The antibacterial activity of βs and their metal complexes were screened against thirteen gram-positive and twenty gram-negative bacteria and their names are listed along with the notations (see Fig. 5-8). The graph is plotted for the observed values of the zone of inhibition and MIC against the active gram-positive bacteria for βs and their metal complexes as shown in Fig. 5 (a, b). The ligand (βs) is effective against six gram-positive bacteria with a zone of inhibition ranging between 11-18 mm (MIC = 92-100 mg/mL). The βs- Mg complex showed good activity against three gram-positive with a zone of inhibition ranging from10-18 mm (MIC = 110-160 mg/mL). Whereas the complex βs- Ni was found to be the most active as it showed the highest antibacterial activity against different types of gram-positive bacteria with a zone of inhibition ranging from 20-24 mm (MIC = 90-96 mg/mL). Furthermore, the βs- Zn complex exhibited good activity against four gram-positive bacteria with a zone of inhibition ranging between 12-18 mm (MIC= 110-164mg/mL).

The plot for the observed values of the zone of inhibition and MIC against the active gram-negative bacteria for βs and their metal complexes are shown in **Fig. 6 (a, b)**. It is observed that βs showed moderate activity against negative bacteria with a zone of inhibition ranging from 10 to 20 mm (MIC values ranging from 90 to 100 mg/mL) and these values are in good agreement with the reported value [41]. The βs- Mg complex showed good activity against three gram-negative bacteria with a zone of inhibition ranging from 18 to 19 mm (MIC values 110 mg/mL). Whereas the complex βs- Ni was found to be the most active against ten negative bacteria with a zone of inhibition ranging from 14 to 33 mm (MIC = 72 to 140mg/mL). Furthermore, the βs- Zn complex exhibited significant activity for four gram-negative bacteria having a zone of inhibition ranging from 11 to 29 mm and corresponding MIC values ranging from 110 to 164 mg/mL.

The synthesized metal complexes were also tested for in vitro antifungal activity (see **Fig. 7** & **8**). The ligand βs are effective against three fungal strains with a zone of inhibition ranging from 7 to 8 mm (see **Fig. 7**) and show MIC values of 100 mg/mL (see **Fig. 8**) for each fungus. The prepared metal complexes showed remarkable activity with their respective zone of inhibition and MIC values. In the yeast βs-Mg complex, the zone of inhibition ranges from 16 to 23 mm (MIC values ranging from 95 to 120 mg/mL). Whereas weak activity was found in dermatophytes and saprophytes with a zone of inhibition values ranging from 10 to 11 mm (MIC =180 to 174 mg/mL). The βs-Ni complex has a zone of inhibition ranging between 12 & 22 mm and MIC values between 82 & 180 mg/mL in the yeast. The βs-Ni complex was found inactive against dermatophytes, but it has remarkable activity in saprophytes with a zone of inhibition ranging between 16 & 19 mm, and MIC values were observed between 96 &142 mg/mL. The βs- Zn complex has a zone of inhibition between 11 & 34 mm and corresponding MIC values between 58 &160 mg/mL against the yeast, and it was found inactive against all the applied dermatophytes. Moderate activity was observed against saprophytes with a zone of inhibition lying between 12 & 16 mm (MIC values between 110 & 126 mg/mL). These results revealed that all the synthesized metal complexes exhibit enhancement in activity as compared to the ligand.

The ligand and its metal complexes were also tested for their antioxidant activity by DPPH assay compared to standard drugs (Ascorbic acid and BHT). The % RSA of ligand and its complexes were shown in **Table 7**. The βs-Ni complex displayed more significant activity than the ligand. However other metal complexes exhibit moderate activity as compared to standard drugs.

Conclusion

The complexes of metal (Mg, Ni & Zn) with β-sitosterol were synthesized to study the biological activities. A comparative study of these complexes has been carried out through various characterization techniques. The IR result showed that ligand (βs) was coordinated with metals through OH and C=C and the octahedral geometry was observed. The TGA result is in good agreement with the spectral and elemental analysis. EDX result showed the desired mass percentage composition of the elements present in the synthesized complexes. The morphological changes for different metals were also observed in the complexes. The change in the texture of samples is due to the interaction of metals with a ligand which arranges them in the fixed geometry. The synthesized metal complexes exhibited more enhancement in activity as compared to βs. Based on the activity results, the βs-Ni complex was found to be the best in

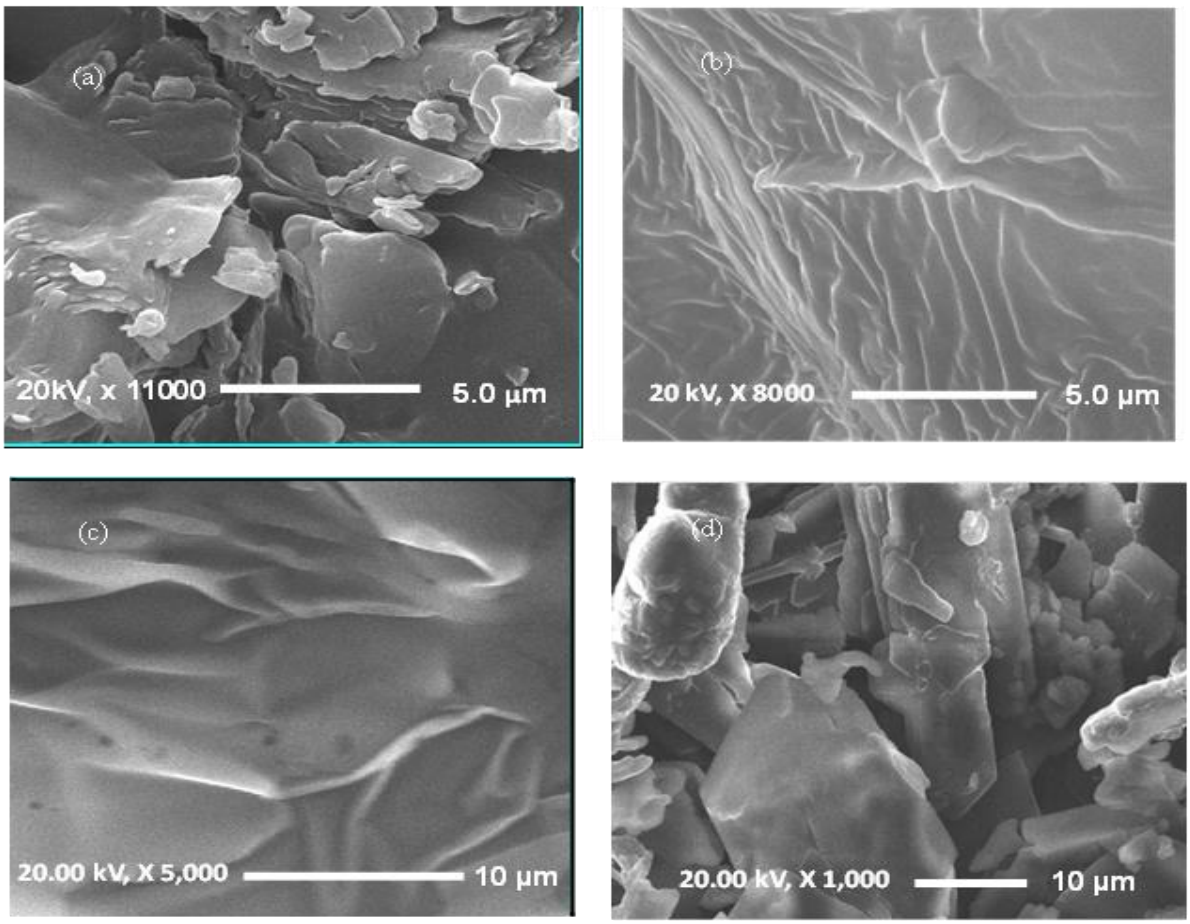

Fig. 3: The SEM results for (a) βs, (b) βs–Mg, (c) βs–Ni and (d) βs–Zn

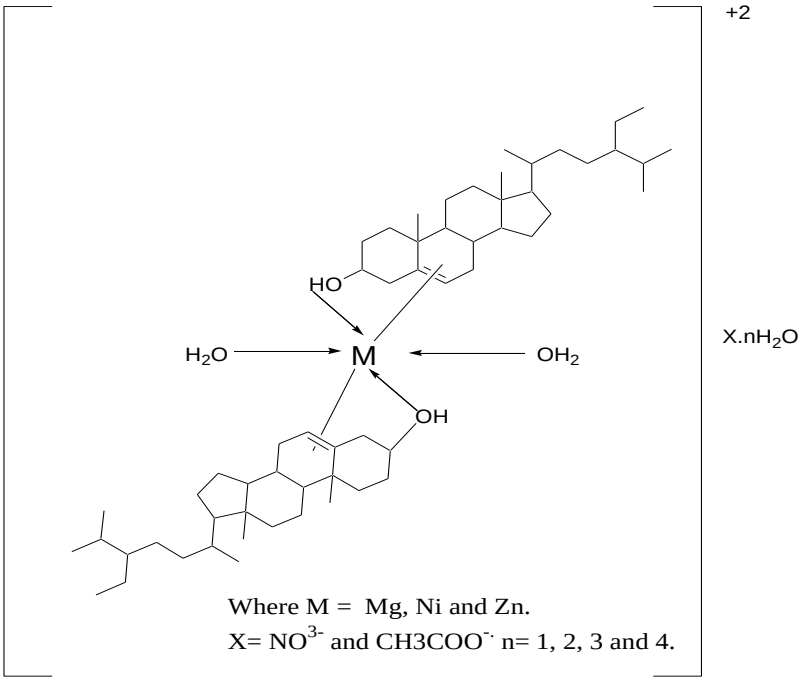

Fig. 4: The Proposed structural formula of sterol metal complexes $ML_2X.nH_2O$

Gram positive bacteria (MIC)
Bacillus cereus (Bc)
Bacillus subtilis (Bs)
Bacillus thruingiensis (Bt)
Corynebacterium diptheriae (Cd)
Corynebacterium hofmanii (Ch)
Corynebacterium xerosis (Cx)
Staphylococcus epidermidis (Se)
Streptococcus saprophyticus (Ss)
M. smegmatis (M.s)
Streptococcus fecalis (Sf)
Streptococcus pyogenes (Sp)

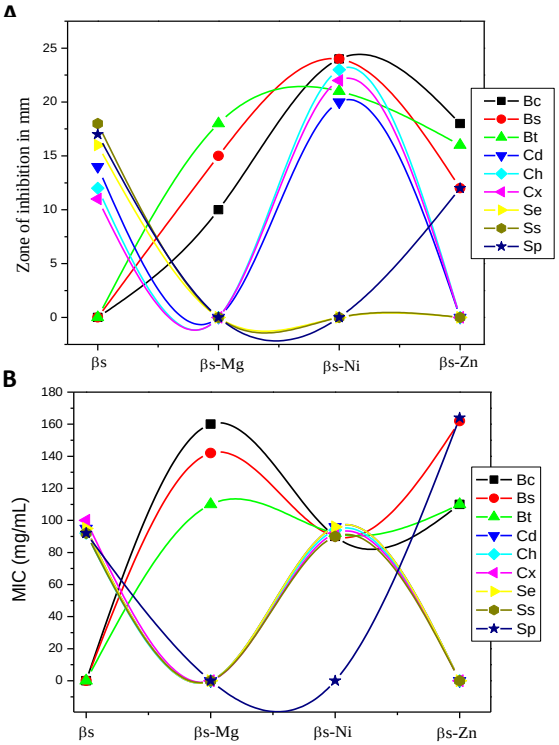

Fig. 5: The plot for **(A)** the antibacterial potential **(B)** the MIC of βs and its complexes against active gram positive bacteria. The list of gram positive bacteria tested for all samples is also provided and graph is plotted for active bacteria only.

Gram negative bacteria
Enterobacter aerogenes (Ea)
Escherichia coli ATCC 8739 (EcA)
Escherichia coli (Ec)
E. coli multi drug resistance (Ecm)
Klebsiella pneumoniae (Kp)
Salmonella typhi (St)
Salmonella paratyphi A (SpA)
Salmonella paratyphi B (SpB)
Shigella dysenteriae (Sd)
Serratia marcesens (Sm)
Acinetobacter baumanii (Ab)
Campylobacter jejuni (Cj)
Campylobacter coli (Cc)
Helicobacter pylori (Hp)
Hemophilus influenzae (Hi)
Vibrio cholerae (Vc)
Aeromonas hydrophila (Ah)
Proteus mirabilis (Pm)
Pseudomonas aeruginosa (Pa)
Pseudomonas aeroginosa ATCC (PaA)

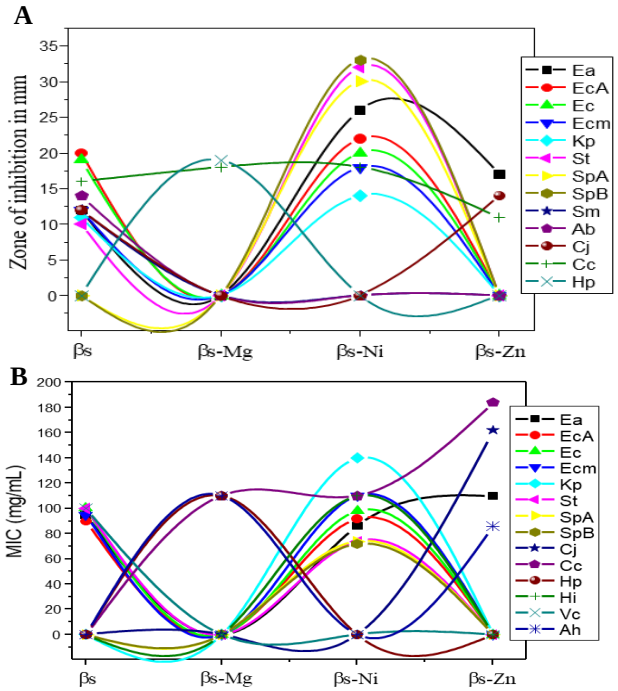

Fig. 6: The plot for **(A)** the antibacterial potential and **(B)** the MIC of βs and its complexes against gram negative bacteria. The gram-negative bacteria tested for all samples are also listed in the table and graph is plotted for the active bacteria only

Yeasts
Candida albicans (Ca)
Candida albicans ATCC 0383 (CaA)
Saccharomyces cerevisiae(Sc)
Candida galbrata (Cg)
Candida tropicalis(Ct)
Candida kruzei(Ck)
Dermatophytes
Microsporum canis (Mc)
Microsporum gypseum (Mg)
Trichophyton rubrum (Tr)
Trichophyton mentagrophytes (Tm)
Trichophyton tonsurans(Tt)
Saprophytes
Aspergillus flavus(Af)
Aspergillus niger (An)
Fusarium specie(As)
Penicillium sp(Psp)
Rhizopus(R)
Helminthosporum (H)

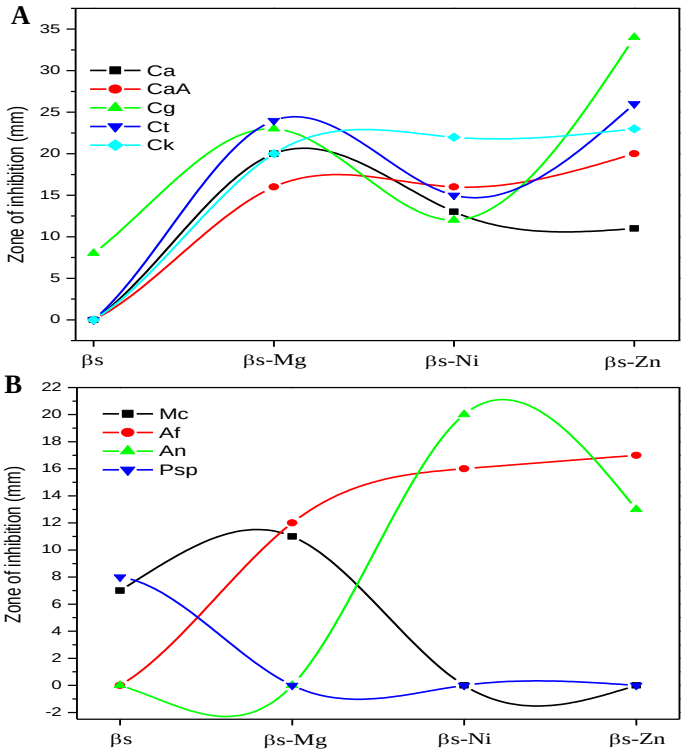

Fig. 7: The plot for the screening of antifungal activity for **(A)** Yeasts and **(B)** Dermatophytes and Saprophytes of βs and its complexes against pathogenic fungi

Yeasts
Candida albicans (Ca)
Candida albicans ATCC 0383 (CaA)
Candida galbrata (Cg)
Candida tropicalis Ct)
Candida kruzei (Ck)
Dermatophytes
Microsporum canis (Mc)
Saprophytes
Aspergillus flavus (Af)
Aspergillus niger (An)
Fusarium specie (Fs)
Penicillium sp (Psp)

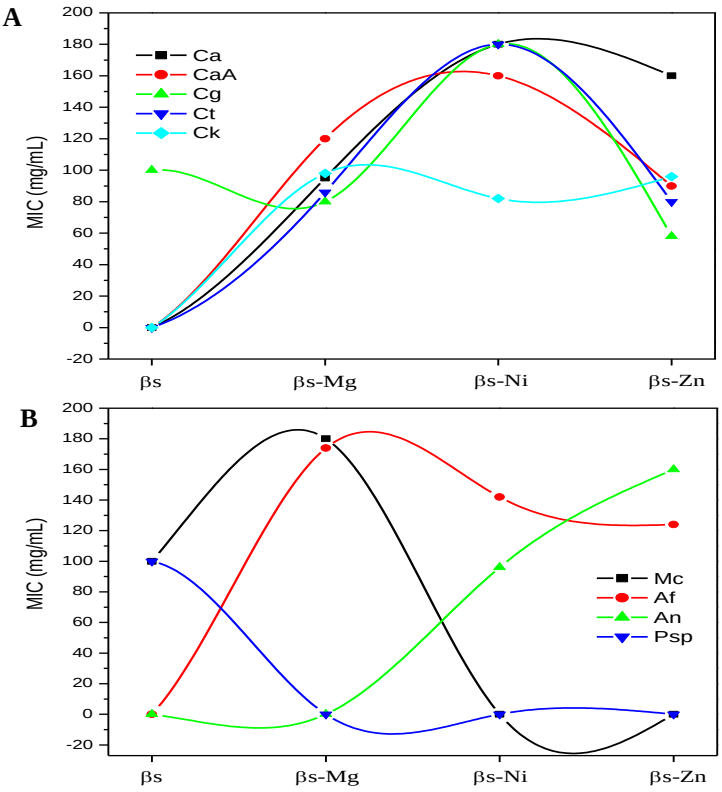

Fig. 8: The plot of MIC values for **(A)** Yeast and **(B)** Dermatophytes and Saprophytes.

Table 7: Antioxidant activities of βs and its complexes

Sr. #	Sample code	RSA%
1	βs	76.20
2	βs-Mg	55.12
3	βs-Ni	87.56
4	βs-Zn	53.45
5	Ascorbic Acid	96.100
6	Butylated hydroxytoulene	75.700

inhibiting the growth of bacteria and exhibited significant antioxidant activity. The results revealed that the synthesized complexes were more potent antimicrobial agents against several bacterial and fungal strains. Furthermore, more clinical trials and scientific evaluation are necessary for these metal complexes to use as antibacterial and antifungal agents after testing their toxicity.

Conflict of interest

The authors declare no conflict of interest.

References

[1] Prakash A, Adhikari D. A Review on Application of Schiff bases and their metal complexes. International Journal of Chem Tech Research 2011;3 (4):1891-1896.

[2] Sun RW, Ma DL, Wong EL, Che CM. Some uses of transition metal complexes as anti-cancer and anti-HIV agents. Dalton Transactions 2007;(43):4884-92.

[3] Ray S, Mohan R, Singh JK, Samantaray MK, Shaikh MM, Panda D, Ghosh P. Anticancer and antimicrobial metallopharmaceutical agents based on palladium, gold, and silver N-heterocyclic carbene complexes. Journal of the American Chemical Society 2007;129(48):15042-53.

[4] Lange TS, Kim KK, Singh RK, Strongin RM, McCourt CK, Brard L. Iron (III)-salophene: an organometallic compound with selective cytotoxic and anti-proliferative properties in platinum-resistant ovarian cancer cells. PLoS One 2008;3(5):2303.

[5] Khan G, Merajver S. Copper chelation in cancer therapy using tetrathiomolybdate: an evolving paradigm. Expert opinion on investigational drugs 2009;18(4):541-8.

[6] Guo Z, Sadler PJ. Metals in medicine. Angewandte Chemie International Edition 1999;38(11):1512-31.

[7] Arish D, Nair M S. Synthesis, characterization and biological studies of Co (II), Ni (II), Cu (II) and Zn (II) complexes with pyrral-L-histidinate. Arabian Journal of Chemistry 2012;5(2):179-186.

[8] Williams CJ, Whitehouse JM. Cis-platinum: a new anticancer agent. British Medical Journal 1979;1(6179):1689.

[9] Jamieson ER, Lippard SJ. Structure, recognition, and processing of cisplatin− DNA adducts. Chemical reviews 1999;99(9):2467-98.

[10] Drumm TD, Gray JI, Hosfield GL. Variability in the major lipid components of four market classes of dry edible beans. Journal of the Science of Food and Agriculture 1990;50(4):485-97.[11] Huang YS, Redden P, Lin X, Smith R, MacKinnon S, Horrobin DF. Effect of dietary olive oil non-glyceride fraction on plasma cholesterol level and liver phospholipid fatty acid composition. Nutrition research 1991;11(5):439-48.

[12] Thorpe CW. Campesterol and β-sitosterol content of some vegetable oils. Journal of the Association of Official Analytical Chemists 1972;55(5):1085-7.

[13] Morton GM, Lee SM, Buss DH, Lawrance P. Intakes and major dietary sources of cholesterol and phytosterols in the British diet. Journal of Human Nutrition and Dietetics 1995;8(6):429-40. [14] Hąc-Wydro K. The effect of β-sitosterol on the properties of cholesterol/phosphatidylcholine/ganglioside monolayers-The impact of monolayer fluidity. Colloids and Surfaces B: Biointerfaces 2013; 110:113-9.

[15] Kim KA, Lee IA, Gu W, Hyam SR, Kim DH. β-Sitosterol attenuates high-fat diet-induced intestinal inflammation in mice by inhibiting the binding of lipopolysaccharide to toll-like receptor 4 in the NF-κB pathway. Molecular nutrition & food research 2014;58(5):963-72.

[16] Baskar AA, Al Numair KS, Gabriel Paulraj M, Alsaif MA, Muamar MA, Ignacimuthu S. β-sitosterol prevents lipid peroxidation and improves antioxidant status and histoarchitecture in rats with 1, 2-dimethylhydrazine-induced colon cancer. Journal of Medicinal Food 2012;15(4):335-43.

[17] Vivancos M, Moreno JJ. β-Sitosterol modulates antioxidant enzyme response in RAW 264.7 macrophages. Free Radical Biology and Medicine 2005;39(1):91-7.

[18] Tao R, Wang CZ, Kong ZW. Antibacterial/antifungal activity and synergistic interactions between polyprenols and other lipids isolated from Ginkgo biloba L. leaves. Molecules 2013;18(2):2166-82.

[19] Shazia R, Muhammad I, Anwar N, Haji A, Amin A. Transition metal complexes as potential therapeutic agents. Biotechnology and Molecular Biology Reviews 2010;5(2):38-45.

[20] Perez C. Antibiotic assay by agar-well diffusion method. Acta Biol Med Exp 1990;15:113-5.

[21] Vaghasiya Y, Patel H, Chanda S. Antibacterial activity of Mangifera indica L. seeds against some human pathogenic bacterial strains. African Journal of Biotechnology 2011;10(70):15788-94.

[22] Smyth RW, Bengtsson S, Cloke J. Performance evaluation of M.I.C. Evaluator™ strip (Oxoid) and comparison with the BSAC reference method. 2008.

[23] Wuthi-udomlert M, Vallisuta O. In vitro Effectiveness of Acacia concinna extract against Dermatomycotic Pathogens. Pharmacognosy Journal 2011;3(19):69-73.

[24] Badarinath AV, Rao KM, Chetty CM, Ramkanth ST, Rajan TV, Gnanaprakash K. A review on in-vitro antioxidant methods: comparisions, correlations and considerations. International Journal of PharmTech Research 2010;2(2):1276-85.

[25] Blois MS. Antioxidant determinations by the use of a stable free radical. Nature 1958;181(4617):1199-200.

[26] Nakamoto K. Infrared spectra of Inorganic and Coordination Compounds. New York: Wiley; 1970.

[27] Nawar N, Hosny NM. Synthesis, spectral and antimicrobial activity studies of o-aminoacetophenone o-

hydroxybenzoylhydrazone complexes. Transition Metal Chemistry 2000;25(1):1-8.
[28] REDDY K RK, Suneetha P, Karigar CS, Manjunath NH, Mahendra KN. COBALT (II), Ni (II), Cu (II), Zn (II), CD (II), Hg (II), U0 (2)(VI) AND th (IV) COMPLEXES FROM ONNN SCHIFF BASE LIGAND. Journal of the Chilean Chemical Society 2008;53(4):1653-7.
[29] Anbu S, Kandaswamy M, Moorthy PS, Balasubramanian M, Ponnuswamy MN. New polyaza macrobicyclic binucleating ligands and their binuclear copper (II) complexes: Electrochemical, catalytic and DNA cleavage studies. Polyhedron 2009;28(1):49-56.
[30] Ghosh S, Malik S, Jain B, Iqbal SA. Synthesis, characterization, antimicrobial and diuretic study of Mg (II), Mn (II), Fe (II) and VO (II) complexes of chemotherapeutic importance. Journal of Saudi Chemical Society 2012;16(2):137-43.
[31] Prasad AS, Fitzgerald JT, Bao B, Beck FW, Chandrasekar PH. Duration of symptoms and plasma cytokine levels in patients with the common cold treated with zinc acetate: a randomized, double-blind, placebo-controlled trial. Annals of internal medicine 2000;133(4):245-52.
[32] Lever ABP, Inorganic electronic spectroscopy, 2nd ed.; Elsevier: Amsterdam; 1984.
[33] Lewis J, Wilkins RG, Modern Coordination Chemistry. New York: Inter science publishers; 1967.
[34] Uddin MN, Salam MA, Sultana J. Pb (II) complexes of Schiff bases derived from benzoylhydrazine as the antibacterial agents. Science publishing group 2015; 3:7-14.
[35] Nair MS, Arish D, Joseyphus RS. Synthesis, characterization, antifungal, antibacterial and DNA cleavage studies of some heterocyclic Schiff base metal complexes. Journal of Saudi Chemical Society 2012;16(1):83-8.
[36] Wahab A, Sultana A, Khan KM, Irshad A, Ambreen N, Ali M, Bilal M. Chemical investigation of Xanthium strumarium Linn and biological activity of its different fractions. Journal of Pharmacy Research 2012;5(4):1984-7.
[37] Chohan ZH, Pervez H, Rauf A, Khan KM, Supuran CT. Isatin-derived antibacterial and antifungal compounds and their transition metal complexes. Journal of Enzyme Inhibition and Medicinal Chemistry 2004;19(5):417-23.
[38] Mony A, Vinila VS, Jacob R, Nair HG, Issac S, Rajan S, Isac J. Thermal Behaviour of Nano Crystalline Ceramic PbSrBaTiO. International Journal of Innovative Science, Engineering & Technology 2014;1(10).
[39] Patel R, Garg R, Erande S, Maru GB. Chemopreventive herbal anti-oxidants: current status and future perspectives. Journal of clinical biochemistry and nutrition 2007;40(2):82-91.
[40] Al-Qadasy MK, Al-Azab FM, Al-Maqtari MA, Jamil YM. Spectroscopic and Antibacterial Studies of Mixed Ligand Complexes of Transition Metal (II) Ions with Sulfadoxine and 1, 10-Phenanthroline. PSM Biol. Res 2018;3(1):16-28.
[41] Bumrela S B, Naik S R. Identification of beta-carotene and beta-sitosterol in methanolic extract of Dipteracanthus patulus (Jacq) nees and their role in antimicrobial and antioxidant activity. International journal of Phytomedicine 2011;3(2):204.